Journal of the Korea Convergence Society
Vol. 7. No. 4, pp. 181-190, 2016
http://dx.doi.org/10.15207/JKCS.2016.7.4.181

Preliminary Development of Pinwheel Model Created by Convergent Truss Structure with Biological DNA Structure

Jeongho Choi
Aircraft Design and Development Department, Korea Aerospace Industries LTD

생물학적 DNA 구조와 트러스구조의 융합으로 개발한 바람개비형 모델 선행연구

최정호
한국항공우주산업주식회사 기체설계팀

Abstract The objective of this study is to find the effective stiffness and compressive strengths of a unit-cell pinwheel truss and double pinwheel truss model designed following a double helical geometry similar to that of the DNA (deoxyribonucleic acid) structure in biology. The ideal solution for their derived relative density is correlated with a ratio of the truss thickness and length. To validate the relative stiffness or relative strength, ABAQUS software is used for the computational model analysis on five models having a different size of truss diameter from 1mm to 5mm. Applied material properties are stainless steel type 304. The boundary conditions applied were fixed bottom and 5 mm downward displacement. It was assumed that the width, length, and height are all equal. Consequently, it is found that the truss model has a lower effective stiffness and a lower effective yielding strength.

• Key Words : coiled wires, DNA, double helix, helical geometry, micro-lattice, truss

1. Introduction

Lightweight models such as honeycomb, open cell, closed cell have been studying more and more in these days. For decades, scientists and researchers have been attempting to find or create an advanced model. At present, the truss model shows promise as a structure for creating a lightweight model with effective heat protection structure or high strength. For example, the metallic micro-lattice is one of the lattice structures developed [1] which is strong, of low density, stiff, and lightweight[2,3,4]. The development of lattice structures is an interesting subject.

For a long time, scientists have been attempting to create a new lattice model which is lightweight, of low density, and stiff. However, none of these studies considered applying biological concepts such as the DNA's duplex helix for designing a truss model. The DNA structure was discovered by James D. Watson in 1968. The idea of developing a double helix truss (DHT) model was inspired by the double helix structure of a nucleic acid in molecular biology. The

*Corresponding Author : Jeongho Choi(choicaf@gmail.com, jungho.choi@koreaaero.com)
Received June 30, 2016 Revised July 4, 2016
Accepted August 1, 2016 Published August 31, 2016

double helix structure is shown in Fig. 1 [5]. The double helix configuration can be applied in several fields of science and engineering. In the mechanical engineering field, a well-known example is the helix bridge in Singapore. It is the first bridge in the world to use the helix shape as part of its structural design. The function of the helical shape is to provide multiple supports across the gap as shown in Fig. 2 [6,7].

The other examples of the application of the double helix are the crystal structure of a folded molecular helix[8], a natural left-handed helix created by a climber plant[9], a charged particle in a uniform magnetic field follow ing a helical path[10], a helical coil spring[11], an iso truss carbon fiber light weight bicycle[12], mascara (which is a cosmetic product)[13], screw propeller in the ship industry, stair case in architecture, screw pump, etc.

[Fig. 1] Double helix structure [3,14]

The double helical structure is not suitable for application in the development of a unit-cell model of open-cell periodic cellular solid structures such as metallic micro-lattices. In addition, the configuration of the DNA is not enough to be studied for an effective stiffness or effective strength about the open-cell periodic cellular solids based on the general helical geometry. Thus, we decided to develop a new unit-cell model based on the double helical structure and to validate with structural analysis [15.16,17].

[Fig. 2] Helix Bridge in Singapore [5, 8, 18]

The objective is to develop a double helical structure with high stiffness, high strength, and high energy absorption capability similar to a lattice model or a lightweight structure. The disadvantage that this structure is likely to have are its bending/buckling behavior at points that cannot be predetermined and the high level of intricacy involved in the development of a realistic unit model based on the helical structure, which is likely to have a complex structure. Moreover, to create a specimen manually is difficult.

This study is focused on developing an advanced ideal solution incorporating the double helical structure. Therefore, this study defines a unit-cell model created on the basis of the helical structure which is a neo development and obtains the effective stiffness or effective strength. In addition, the model is validated using Gibson-Ashby's ideal solution.

2. Background

2.1 General helix geometry [12] and fundamental idea

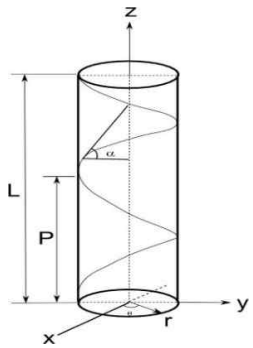

[Fig. 3] General helix geometry

A general helix geometry is based on the equations given below:

$$x=r\cos(t) \quad (1)$$

$$y=r\sin(t) \quad (2)$$

$$z=P\ \theta/2\pi \quad (3)$$

$$a=P/2\pi r \quad (4)$$

$$\omega=L/P \quad (5)$$

where t varies from 0 to π over the length of the

bridge, r is the radius, and list heleng th of the bridge As shown in the figure, the helical geometry can have several parameters and has a circular configuration. Thus, because the helical geometry is complex, it approximates the unit model of the double helical geometry with a rod beam to derive its relative density.

Thus, using the basic model shown in Fig. 4, this approximation creates a new type of structure, which is shown in Fig. 5, and is defined as a pinwheel truss model.

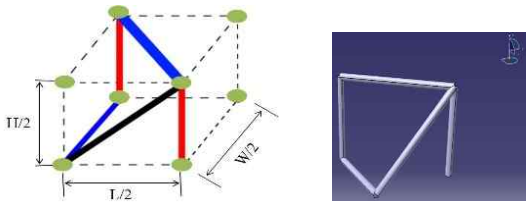

[Fig. 4] Basic idea (left) and a basic model (right) designed by CATIA

2.2 Relative density of pinwheel truss

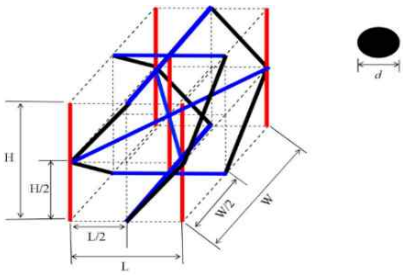

[Fig. 5] Schematic unit model of a double pinwheel truss which is composed of three kinds of struts (red: straight strut, blue: crossed strut, black: helical strut, dot-line: boundary line)

$$\rho/\rho_s \propto V_s/V \quad (6)$$

$$V_s = V_{Vertical} + V_{horizontal} + V_{helix} \quad (7)$$

$$V_{Vertical} = ((\pi d^2)/4)5H \quad (8)$$

$$V_{horizontal} = ((\pi d^2)/4)(2(L+W)+2) \quad (9)$$

$$V_{helix} = ((\pi d^2)/4)[2(2(/2))+2(2(/2))] \quad (10)$$

$$V^* = LWH \quad (11)$$

$$\therefore \rho/\rho_s \propto V_s/V^*$$

$$= (\pi d^2/4)[5H+2(L+W)+2+4]/LWH \quad (12)$$

If $L=W=H=l$, where l is a common parameter, then

$$\rho/\rho_s = ((9+6)/4)\pi(d/l)^2 \quad (13)$$

$$\therefore \rho/\rho_s \propto C \cdot (d/l)^2 \quad (14)$$

where C is a constant and d is a thickness of truss. Thus, relative density is correlated with the ratio of wire diameter to the width, length, or height when all of these are equal to a constant l. Fig. 6 shows the model of a double pinwheel truss which is equivalent to that in Fig. 4. Fig. 7 is a pinwheel truss model from three different views such as isotropic view, top view, left view, and right view.

Essentially, the double pinwheel truss is made of two layers of a pinwheel truss in the vertical direction. In Fig. 6, the top trusses are placed on crossed struts in the middle, which are colored blue, and the top part mirrors the bottom trusses. In addition, the pinwheel truss structure shown in Fig. 6 is composed of two of pinwheel truss structures that are vertically mirrored. Therefore, a stiffness and strength for the unit cell of the double pinwheel and a single pinwheel structure can be expected ideal solutions.

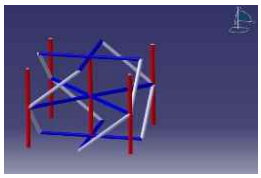

[Fig. 6] Designed a unit-cell model of a double pinwheel truss (red: straight struss, blue: horizontal truss, white: diagonal truss)

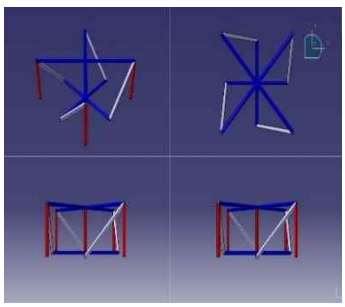

[Fig. 7] Three points of views for a pinwheel truss which is a unit model to make the double pinwheel truss: (top left) isotropic, (rtop right) top view, (below left) left view, (below right) right view

2.3 Relative elastic modulus

The relative modulus is based on an ideal solution defined by Gibson-Ashby [19], i.e., the modulus is

proportional to an exponent of the relative density. However, the exponent of the relative density depends upon the type of the unit cell or the applied material property. Thus, relative modulus is correlated with the ratio of density to the exponent of n.

$$E^*/E_s=C_1(\rho^*/\rho_s)^n \quad (15)$$

where n=2 for rectangular truss model, is an elastic modulus for the model, is an elastic modulus of the applied material $\rho*$ is a density of foam itself, ρ_s is a density of the applied material, and C_1 are constant. In the equation, when the value of the exponent is 2, the unit cell type is an open-cell truss structure having the shape of a regular hexahedron. Thus, based on the equation, we can predict the effective stiffness of a single pinwheel or a double pinwheel truss using finite element analysis, which can find the value of the exponent for the pinwheel truss model.

2.4 Relative strength

To predict the effective compressive strength of a cubic truss model, we use an equation derived from the open cell created by Gibson-Ashby.

$$\sigma^*/\sigma_s=C_2(\rho^*/\rho_s)^n \quad (16)$$

where n is the value of the exponent for a rectangular truss model, σ^* is a compressive yield strength of the model, σ_s is a compressive yield strength of the applied material, $\rho*$ is a density of foam itself, ρ_s is a density of the applied material, and C_2 is a constant. That is, the value of the exponent depends on the shape of the unit cell model. For example, when the value of the exponent is 1.5, the shape of the unit cell is that of a cubic truss. Thus, by varying the exponent, we can predict the effective strength using finite element analysis on a pinwheel truss or a double pinwheel truss.

2.4.1 Relative strength at 25% strain

In addition, using the same equation, we can predict the effective strength at 25% elongation. Thus, equation (16) is to be modified as equation (17).

$$\sigma_{0.25}/\sigma_s=C_3(\rho^*/\rho_s)^n \quad (17)$$

where n is a number of exponent for rectangular truss model, $\sigma_{0.25}$ is the normal plastic collapse occurs at 25% strain and C_3 are constant. When n is 1.5, the unit-cell model has the shape of a regular hexahedron. Thus, we can predict the effective strength of a pinwheel truss or a laminated pinwheel truss at 25% strain.

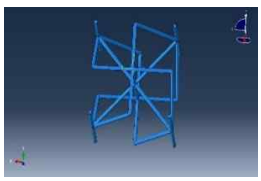

[Fig. 8] Double pinwheel truss defined as fourfold helical truss as top view

3. Simulation

3.1 Quasi static compression

We used ABAQUS v6.11 software for finite element analysis. For simple finite element analysis of a helical truss model having a curvature line, we assume the helical truss to be a straight strut. The fourfold helical truss model is made of two pinwheel trusses, i.e., the bottom pinwheel truss is connected to the top pinwheel truss, which is rotated by 45° about a center bar along the z-axis as shown in Fig. 9.

3.2 Unit model

Applied model is five kinds depending on a size of truss diameter, d, is ranged from 1mm to 5mm as 1mm increment. The width, length, and height are fixed as 20mm for the fourfold truss model shown in Fig.9.

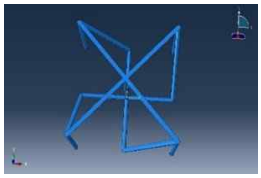

[Fig. 9] A pinwheel truss unit model as top view

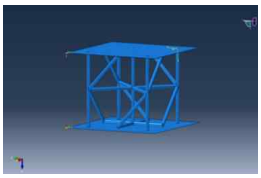

[Fig. 10] Boundary condition for a pinwheel truss which is a unit model to make a fourfold helical geometry (Bottom surface: Ux = Uy = Uz = 0, Rx = Ry = Rz = free; Top surface: Ux = Uz = 0, Uy = 5 mm downward, Rx = Ry = Rz = free)

Thus, for the pinwheel truss model, the applied length and width are equal to 20mm. However, the height is 20mm, because it is half the height of the fourfold truss model shown in Fig.10.

3.2.1 Meshing

The applied general conditions are listed in Table 1. It is a static analysis of the mesh type C3D10. The material used is AISI304 stainless steel of initial yielding strength 215 MPa, ultimate strength 505 MPa, density 8.0 kg/cm3,Young's modulus 200GPa, Poisson ratio 0.29, and friction coefficient 0.1.

<Table 1> General conditions

Simulation code	ABAQUS/static
Material property	AISI304 stainless steel
Mesh type	C3D10
Friction coefficient	0.1
Density(kg/cm^3)	8.0
Young's modulus (GPa)	200
Poisson ratio	0.29
Initial yielding strength (MPa)	215
Ultimate strength(MPa)	505

The applied mesh type is C3D10, and each model has a different total number of nodes and elements, which are listed in Table 2. Each model, of different diameters including 1 mm, 2 mm, 3 mm, 4 mm, and 5 mm, has a different total number of nodes and elements. In addition, to analyze each model, the size of the increments varies from 0.5 mm to 1.3 mm. Thus, the maximum number of increment steps is 1000, when increment size is 0.1.The size of the increment is ranged from 1e-5 as minimum to 0.1 as maximum.

<Table 2> Applied nodes and elements

Diameter d (mm)	Nodes	Elements	Size of increment (mm)
1	58,845	33,133	0.5
2	33,064	18,891	1.1
3	35,825	21,529	1.2
4	38,822	23,768	1.2
5	40,294	25,030	1.3

3.3 Boundary condition

The applied boundary condition is simple—the bottom surface is fixed and the top surface moves downward by 5 mm (vertical direction). This is used to measure the reaction force at the bottom. Fig. 11 shows the pinwheel model and the boundary condition. Rotation over both the top and bottom surfaces is free.

3.4 Simulation for elastic and yielding stress

An analysis of computational models as five different configurations is shown. Basically, simulated models are of different truss diameters—1 mm thru 5 mm—within a space that is fixed at 4 mm.

As can be observed in each figure, the common result among the five models is that the straight vertical truss displays maximum stress while the middle trusses display different distributions of stress. In other words, as the vertical truss deforms, the middle trusses provide support for it to resist this deformation. The main reason behind this is the size of the space. For example, Fig. 12(a) shows the vertical truss as having a stress distribution while the middle trusses do not show as having many stress distributions. Fig. 12(b) to (e) show the middle trusses to have widely spread stress distributions. This indicates that as diameter increases, stress distributions spread widely, i.e., the space size is reduced as diameter increases for a fixed length. Thus, Fig. 13 shows the effective stress as a function of effective

strain. As wire diameter increases, the effective stress, elastic modulus, and yielding strength increase.

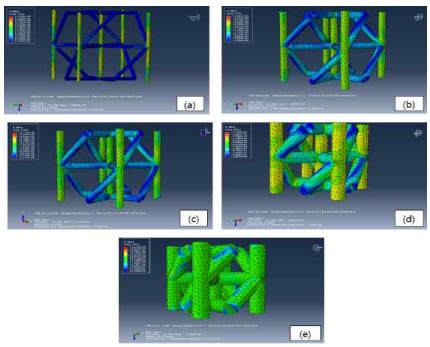

[Fig. 11] Maximum compressive yielding stress for pinwheel truss: (a) d=1mm; (b) d=2mm; (c) d=3mm; (d) d=4mm; (e) d=5mm.

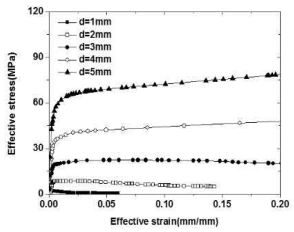

[Fig. 12] Effective Strain-Stress curve

3.5 Simulation for ultimate strength

We conducted simulation for measuring the ultimate strength of the five models of truss diameters varying from 1 mm thru 5 mm as shown in Figure 14(a) thru (e).

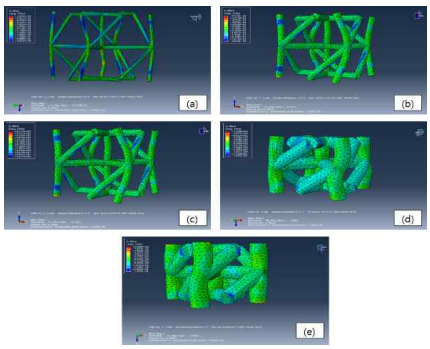

[Fig. 13] Ultimate strength for a pinwheel truss: (a) d=1mm; (b) d=2mm; (c) d=3mm; (d) d=4mm; (e) d=5mm.

At the ultimate strength of all the models, both the vertical trusses and middle trusses are bent. In addition, middle trusses are twisted and moved circularly. Moreover, in all the models, stress is spread over both the vertical and middle sections. The reaction force as a function of displacement is shown in Fig. 15. As truss diameter increases, the reaction force increases.

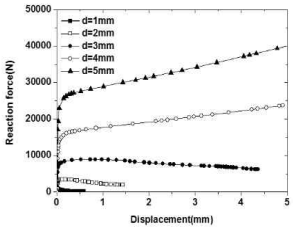

[Fig. 14] Reaction as a function of displacement

3.5.1 Experimental Assessment

To verify the ideal solution of the pinwheel unit model, the five computational models are tested using ABAQUS software.

Essentially, the relative modulus and relative compressive yielding strength are correlated with relative density following Gibson-Ashby theory. Each model has a different diameter from 1 - 5 mm. In the simulation testing, the elastic modulus, compressive yielding strength, and compressive strength at 25% strain for each are determined.

<Table 3> Simulated results of pinwheel truss model

d (mm)	ρ^*/ρ_s	E^* (GPa)	E^*/E_s	σ^*/σ_s	$\sigma_{0.25}/\sigma_s$
1	0.010	25.5	0.001	0.004	0.002
2	0.043	1.44	0.003	0.023	0.022
3	0.098	3.08	0.014	0.074	0.072
4	0.174	5.14	0.023	0.127	0.275
5	0.273	27.5	0.127	0.198	0.624

Based on these parameters, the relative modulus, relative compressive yielding strength, and relative compressive strength at plastic range for each model are calculated and summarized in Table 3.

It can be observed that as diameter increases, the relative modulus, relative compressive yielding strength, and relative compressive strength in the plastic range increase.

5. Results

Using the simulation, the model of the pinwheel truss unit shape is tested. It is observed that the values of elastic modulus, compressive strength at yielding, and compressive strength in the plastic range are corrected by computational analysis. For each model, of the pinwheel, these parameters are plotted on a log-log scale and compared with the ideal solution provided by Gibson-Ashby. In the ideal solution by Gibson-Ashby, the relative elastic modulus is correlated with the relative density using the second power law. The relative strength is correlated with the relative density as three over two in the power law. This is shown as a solid line in Fig. 15 for the relative Young's modulus, Fig. 16 for the relative compressive yielding strength, and Fig. 17 for the relative compressive strength at 25% strain. The simulated results for the pinwheel truss models shown in Figs. 15 - 17 are defined as the rectangular dot shape. In the case of the fourfold truss, the simulated results shown in Figs. 15 - 17 are defined as the diamond dot shape. The relative Young's modulus as a function of relative density is shown in Fig. 15. The ideal solution obtained for the fourfold truss models is such that the relative Young's modulus is equal to the constants multiplied by the relative density raised to the power 1.34. The pinwheel truss models proved that the relative Young's modulus is correlated to constants multiplied to the relative density to the power 1.1. Thus, both models show a lower elasticity than that of the ideal solution of Gibson-Ashby. The relative compressive yielding strength as a function of relative density is shown in Fig. 16. The ideal solution obtained for the fourfold truss models is such that the relative Young's modulus is equal to the constants multiplied by the relative density raised to the power 0.83.

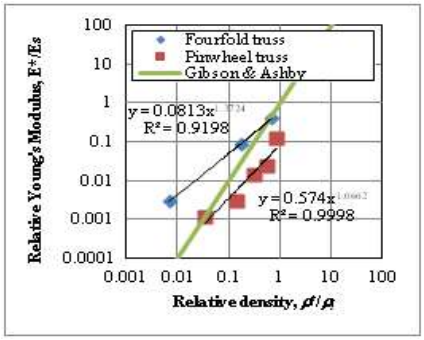

[Fig. 15] Relative Young's modulus as a function of relative density

The pinwheel truss models prove that the relative Young's modulus is correlated to the constants multiplied by the relative density raised to the power 1.1. Thus, both the models display a slightly lower compressive yielding strength than that of the ideal solution of Gibson-Ashby. The relative compressive strength at 25% strain as a function of the relative density is shown in Fig. 17. The ideal solution obtained for the fourfold truss models is such that the relative compressive strength at 25% strain is equal to the constants multiplied by the relative density raised to the power 1.17.

The pinwheel truss models prove that the relative compressive strength at 25% strain is correlated to the constants multiplied to the relative density raised to the power 1.71. Thus, the fourfold truss models display a slightly lower compressive strength than that of the ideal solution of Gibson-Ashby. However, the pinwheel truss models display a higher compressive strength than that of the ideal solution of Gibson-Ashby.

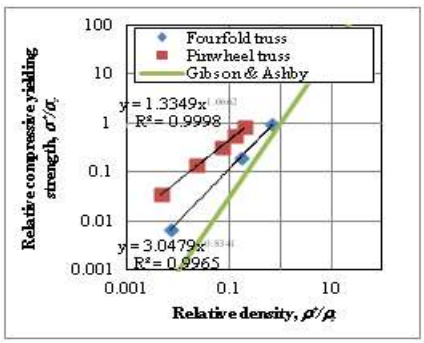

[Fig. 16] Relative compressive yielding strength as a function of relative density

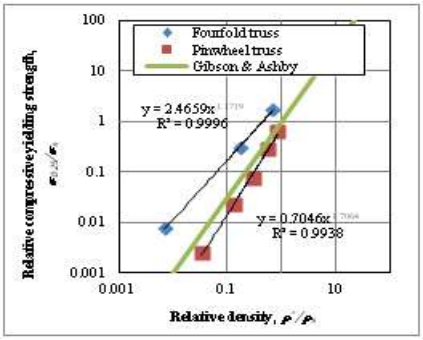

[Fig. 17] Relative compressive strength at 25% strain as a function of relative density

6. Discussion

We have analyzed a pinwheel truss model to measure its three characteristics relative modulus, relative compressive yielding strength, and relative compressive strength at 25% strain. The main aim of the analysis is to validate the pinwheel truss models by comparing them to Gibson-Ashby's ideal solution with regard to the three characteristics. From the analysis of the relative elastic modulus, we determined that the pinwheel truss model has a lower elasticity than that of the ideal solution of Gibson-Ashby. The main reason behind this result is that the outer vertical truss of the pinwheel can easily bend to support the stress applied over the top surface and follows a rotational movement for a thicker truss diameter. This implies that the pinwheel model begins to move in one direction in a manner similar to a pinwheel movement. Essentially, if stress is applied over the top surface, it will initially impact the pinwheel truss at the outer vertical truss. Then, the applied stress shifts to the middle truss. The middle truss is set downward in the shape of a pinwheel.

Therefore, the truss is called a pinwheel truss model. With respect to the relative yielding strength, the pinwheel truss model also displays a compressive yielding strength lower than that of the ideal solution. The main reason behind this is similar to that in the previous description about relative modulus. The outer truss can be affected initially. In the following stage, the middle point connected with the horizontal truss begins to bend. Therefore, we conclude that the compressive yielding strength is lower. Lastly, the relative strength at 25% strain displays a value higher than that of the ideal solution. The main reason behind this is that the strength in the 25% plastic range can have a higher value as the truss diameter increases within the constant space size. The middle trusses also bend and buckled at the same time. Thus, the relative compressive strength in the plastic range displays a value higher than that of the ideal solution based on the theory of Gibson-Ashby. Using the finite element model analysis, we can predict that the exponent of the relative density of the pinwheel truss model when correlated with its relative elastic modulus is approximately 1.1. This implies that the truss model has an effective stiffness similar to that of a honeycomb structure, i.e., the effective stiffness of the honeycomb structure is 1 and that of the pinwheel truss model is approximately 1. Moreover, a pinwheel truss can have a higher effective stiffness than that of a double pinwheel truss as truss thickness increases. The effective strength of the double pinwheel truss at initial yielding point is also correlated with the relative density by approximately 1.1. This indicates that the double pinwheel truss model may have strength approximately equal to that of the honeycomb. Moreover, the effective initial yield strength of the truss is higher than that of the pinwheel truss as truss thickness increases. The effective strength at 25% strain, the plastic strength, is correlated with an exponent of the relative density of about 1.7. This means that the truss model has an effective strength approximately equal to that of an open-cell rectangular model defined by Gibson and Ashby. Essentially, we have determined that the truss model has a lower effective stiffness and a lower effective yielding strength. However, the truss model has a higher effective strength at the field of plasticity.

7. Conclusions

The idea of a pinwheel truss model is derived from the double helix structure of the DNA. It is the result of a fusion between engineering analysis and biological concept. As can be observed from the previous results, the pinwheel truss model does not possess a reasonably high elasticity and compressive yielding strength. However, it possesses a better compressive strength in the field of plasticity. Therefore, the pinwheel truss structure needs to be developed further to obtain higher effective elasticity and effective yielding strength. In future, it is hoped that real models made using advanced technology such as 3D printing [20,21,22] will be developed and that they will undergo precision testing. Moreover, the pinwheel truss model can be developed for application in a sandwich core and the Aerospace or ship manufacturing industry. It is hope that biological concpets converged with a new open cell structure can be developed more and more [23].

REFERENCES

[1] T. A. Scjaedler, “Ultralight metallic microlattices”, Sci., Vol. 334, pp. 962-965, 2011.

[2] Ultralight, Ultrastiff, “Mechanical Metamaterials”, Sci., Vol. 344, pp. 1373-1377, 2014

[3] J. B. Ma, J. I. Lee, “Mechanical Characteristics Analysis of Structural Light-weight Aluminum Foam”, Journal of the Korea Convergence Society, Vol. 2, No. 3, pp. 1-6, 2011.

[4] Jung-Ho Lee, Jae-Ung Cho, “Study on the Convergent Life Evaluation due to the Bumper Configuration of Multipurpose Vehicle ”, Journal of the Korea Convergence Society, Vol. 6, No. 5, pp. 85-90, 2015.

[5] J. D. Watson, “A Structure for Deoxyribose Nucleic Acid”, Nature, Vol. 171, pp. 737-738, 1953.

[6] C. Huang, "Marina's pedestrian bridge named "The Helix", vehicular bridge named "Bayfront Bridge"". Channel News Asia. Retrieved 23 April 2010.

[7] T. Carfrae, L-M. See, “The Helix Footbridge”, Proceedings of the Conference on Structural Marvels, Singapore 2010.

[8] D. Jason, “The use and optimization of the helix shape as the primary structural element in the design of a steel bridge”, Thesis, Albert Nerken School of Engineering, 2012.

[9] E. G. Carayannis, D. F. J. Campbell, “Mode 3 knowledge production in quadruple helix innovation systems: 21st-century democracy”, innovation, and entrepreneurship for development. Springer, NY, USA, 2012.

[10] J.-L. Schmitt, “Helicity encoded molecular strands”, Helv. Chim. Acta, Vol. 86, pp. 1598-1624, 2003.

[11] S. Isnard, W. K. Silk, “Moving with climbing plants from Charles Darwin’s time into the 21st century”, Ameri. J. Botany, Vol. 96, No. 7, pp. 1205-1221, 2009.

[12] J. L. Robert, L. M. David, P. L. Robert, H. A. Mario, “Electron reflectometry in the martian atmosphere”, Icarus, Vol. 194, pp. 544-561, 2008.

[13] J. Park, S. Chon, J. Lee, K. Sung, and S. Song, “Digital Filter Model for Analog Helical Coil Spring Reverberator”, The Journal of the Acoustical Society of Korea, Vol.25, pp. 291-297, 2006.

[14] Gi-Chul Yang, “Integration Scheme of Gene Information based on Anatomical Structure”, Journal of digital Convergence , Vol. 13, No. 2, pp. 153-158, 2015.

[15] Jung-Ho Lee, Jae-Ung Cho, “Study on Convergence Technique due to the Shape of Cruiser Board through Structural Analysis”, Journal of the Korea Convergence Society, Vol. 6, No. 4, pp. 99-104, 2015.

[16] Jung-Ho Lee, Jae-Ung Cho, “Study on Convergence Technique through Structural Analysis due to the Configuration of Guitar”, Journal of the Korea Convergence Society, Vol. 6, No. 4, pp. 9-14, 2015.

[17] Man Soo Koh, Soon Ki Kwon, Soek Lee, Gil, “A Study for the Dynamic Characteristics and

Correlation with Test Result of Gantry Robot based on Finite Element Analysis“, Journal of the Korea Convergence Society, Vol. 13, No. 1, pp. 269-274, 2015.

[18] Usineviciu, “Bridges conference”, Mathematical Art Gallerries, 2013.

[19] L. J. Gibson, M. F. Ashby, “Cellular Solids: Structure and Properties”, Cambridge University Press, 1999

[20] Sung-Ho Kim, “Development of the 3D Hair Style Simulator using Augmented Realityd“, Journal of the Korea Convergence Society, Vol. 6, No. 6, pp. 249-255, 2015.

[21] Young-Joon Jeong, Sang-Hyun Kim, “Useful evaluation of 3D target location correction by using Xsight spine tracking system in CyberKnife“, Journal of the Korea Convergence Society, Vol. 13, No. 1, pp. 331-339, 2015.

[22] Wan-Bok Lee, “Mesh Cutting Method for 3D Model”, Journal of digital Convergence , Vol. 13, No. 4, pp. 303-310, 2015.

[23] Cheon-Woong Park, Jun-Woo Kim, “An Empirical Research on Information Privacy and Trust Model in the Convergence Era”, Journal of digital Convergence, Vol. 13, No. 4, pp. 219-225, 2015.

저자소개

최 정 호 (Jeongho Choi) [정회원]

・2005년 5월 : Embry-Riddle Aeronautical University, Master of Science in Aerospace Engineering (항공우주공학석사)

・2010년 12월 : The University of New South Wales, PhD in Aerospace Engineering (항공공학박사)

・2011년 4월 ~ 2012년 11월 : 한국재료연구소 선임연구원

・2015년 1월 ~ 현재 : 한국항공우주산업주식회사 선임연구원

<관심분야> : Cellualr solids, Lightweight structure